THE JOURNAL OF PHYSICAL CHEMISTRY B LETTERS

2007, *111,* 8713−8716
Published on Web 06/29/2007

Formation of Viscoelastic Protein Droplets on a Chemically Functionalized Surface

S. Belegrinou, I. Mannelli, L. Sirghi, F. Bretagnol, A. Valsesia, H. Rauscher,* and F. Rossi

Institute for Health and Consumer Protection, European Commission Joint Research Centre, V. Fermi 1, 21020 Ispra, Italy

Received: April 30, 2007; In Final Form: June 14, 2007

Droplet formation during adsorption of the protein lactoferrin from an aqueous solution on a surface functionalized by plasma deposited poly(acrylic acid) is studied using quartz crystal microbalance and atomic force microscopy. The formation of protein droplets is particularly favored at pH values close to the isoelectric point of lactoferrin, where the molecules carry little excess charge and intermolecular attraction exceeds the molecule−surface interaction. By combining topographic data with information on the system dynamics, it is possible to describe the viscoelastic properties of the adsorbate within a quantitative model for nonhomogeneous layers.

The general interest in the interaction of proteins and other biomolecules with functionalized surfaces that allow control and/or modification of adsorption under well-defined conditions arises from many possible applications such as the development of biosensors and biomedical or bioanalytical applications.[1−4] Understanding the dynamical and structural properties of protein layers on such surfaces, and the resulting macroscopic characteristics of the system, is a key necessity to fully exploit their potential in different applications.

Dynamic properties such as the viscoelasticity of adsorbed layers that are formed by adsorption of biomolecules from a solution can be studied online using the quartz crystal microbalance (QCM). By monitoring simultaneously the frequency and the dissipation shifts of the quartz sensor, information can be gained on processes that proceed during the formation of the film such as spreading, structural changes, and more.[5−7] QCM data are currently widely used in many multidisciplinary studies that include interactions between biomolecules and surfaces. It is therefore of paramount importance to realize when standard analysis of those data cannot be applied and hence additional information that is complementary to the viscoelastic data is necessary to understand the behavior of the adsorbate−substrate system.

In the following, we show that, for a correct interpretation of viscoelastic data, it can be of key importance to combine those data with additional information on the topography of the layer at different stages of formation. This is because, in the standard quantitative analysis of the viscoelasticity of the adsorbed films (which is often based on the Voigt or Maxwell approaches or combinations thereof[8]), it is assumed most frequently that the adsorbate/sensor system is homogeneous along planes parallel to the quartz crystal surface. The latter is true for many proteins and other biomolecules studied so far on a variety of surfaces, but in general it cannot be taken for granted. Therefore, standard modeling of the viscoelastic data would lead to erroneous results for inhomogeneous adsorbate layers.

* Corresponding author. E-mail: hubert.rauscher@jrc.it.

As an example, we present here a system where the adsorbate does not form a uniform layer. Consequently, the assumption of a homogeneous film to interpret the QCM results is not valid in this case, and a modified viscoelastic model has to be applied to describe the system in a rigorous and quantitative way. In turn, this allows one to gain additional insight into the underlying processes of adsorbate formation. Specifically, we discuss the adsorption of the protein lactoferrin (Lf) on plasma-polymerized, bioactive poly(acrylic acid) (PAA), as part of a larger study on the interaction of proteins with functionalized surfaces. While the viscoelastic data obtained during the adsorption of other proteins used in that study, e.g., bovine serum albumin, lysozyme, and fibronectin, could be quantitatively analyzed under the assumption that a homogeneous layer is formed,[9] the dissipation upon adsorption of Lf showed a rather surprising and anomalous behavior.

The QCM results are therefore complemented by atomic force microscopy (AFM) measurements at the different stages of adsorption. With this additional topographic information, and utilizing a viscoelastic model that specifically takes the nonhomogeneity of the adsorbate layer into account,[10−12] it is possible to interpret the peculiar behavior of the dissipation in the QCM measurements during adsorption of Lf.

All QCM measurements were performed with a temperature-stabilized instrument with dissipation monitoring (QCM-D, model E4) from Q-Sense (Göteborg, Sweden). Shifts of the fundamental resonance frequency (nominally 5 MHz), including up to the 13th overtone, as well as the corresponding shifts in the dissipation, were measured simultaneously. Polished AT-cut and SiO_2-coated sensor quartz discs (Q-Sense model QSX303) were cleaned by sequential immersion in 1 M NaOH, 1 M HCl, acetone, and ethanol for 10 min each. Then they were coated by PAA films prior to exposure of the sample to the protein solution. PAA, which is generally considered as material that promotes protein adsorption,[13] is deposited on the active QCM electrode by pulsed-plasma-assisted chemical vapor deposition (CVD) in a home-built reactor[13] for 1 min at 50 W, 10% duty cycle, and 4 ms on-time. The samples are subse-

10.1021/jp073297x CCC: $37.00

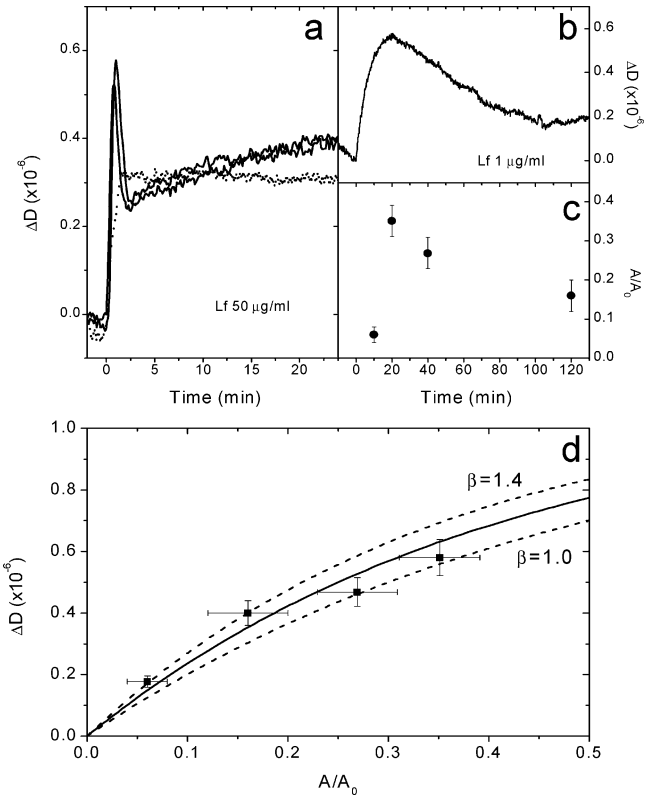

Figure 1. (a,b) ΔD vs time curves during the adsorption of Lf on PAA modified QCM sensors. (a) Solid lines: pH 7.3 and pH 8.62; dotted line: pH 4. Lf concentration $c(\mathrm{Lf}) = 50\ \mu$g/mL. (b) pH 7.3, $c(\mathrm{Lf}) = 1\ \mu$g/mL. (c) Relative area A/A_0 covered by protein droplets as a function of the adsorption time at pH 7.3 and $c(\mathrm{Lf}) = 1\ \mu$g/mL, as measured by AFM. (d) Change in dissipation ΔD vs relative contact area A/A_0. The lines were calculated with the droplet model using eq 3 with β values as indicated.

quently washed for 12 h in MilliQ water and finally dried under nitrogen flow. After introduction in the QCM instrument chamber, the coated sensors were equilibrated with 10 mM phosphate-buffered saline (PBS) solution at different pH until a stable frequency and dissipation baseline signal was reached. The PBS solution was then replaced by a Lf solution (Sigma-Aldrich) in pH-adjusted PBS. After monitoring of the adsorption process, the pure PBS solution was again introduced for rinsing. All measurements were performed at 25 ± 0.02 °C in continuous flow of the solutions, which was maintained by a high-precision peristaltic pump. Because it is known that older-generation instruments can exhibit discontinuities, jumps, or other transients of the QCM signal when the solution is changed, special care was taken to avoid such experimental artifacts. It turned out that with the new generation QCM-D model E4 instrument, the latter was routinely possible under our experimental conditions.

For the AFM measurements, cleaned pieces of a Si wafer were coated with PAA and subsequently rinsed under the same conditions as described above and immersed into the protein solution for the desired time. Then they were washed with PBS solution, dried under nitrogen flow, and immediately analyzed with the AFM (Solver type from NT-MDT Co.).

The formation of a thin homogeneous viscoelastic layer is usually associated with a decrease of the resonance frequency and, in parallel, an increase of the dissipation.[14] However, the adsorption of Lf on PAA does not follow this general trend. Instead, the shift in dissipation vs time during the adsorption of Lf from a 50 μg/mL solution at pH 7.3 and pH 8.62 (Figure 1a) is characterized by a sharp increase immediately when the layer formation starts. For both pH values, the maximum of the dissipation is reached after 1 min, followed by an almost equally steep decrease to a local minimum 80 s after the maximum. After the minimum, the dissipation increases again but at a much slower rate than during the first adsorption phase. A constant dissipation value is reached 60−65 min after the start of the adsorption by slow approach to the saturation value, which is around 0.5×10^{-6} for both pH values and virtually does not change during the final rinsing step. Also, the maximum values differ only slightly for the two pH values. In contrast, the frequency rapidly and monotonously decreases to 90% of its saturation value ($\Delta f \sim 50$ Hz) within the first 2.5 min, i. e., up to the point where the dissipation has the relative minimum, followed by a much slower, further decrease to the final value. The difference in the final value of Δf under these conditions is around 5 Hz for the two pH values. At low pH values around pH 4, however, the characteristic maximum in the dissipation is absent. Rather, the dissipation increases monotonously from the initial to the final value during the adsorption process (see also Figure 1a).

The drastic and unexpected changes of the dissipation during the adsorption process at high pH might be indicative of a structural or morphological transition in the layer.[7] Therefore, we monitored the various adsorption stages, as indicated by the dissipation changes, by AFM as well. For these experiments, we used a Lf solution with lower concentration (1 μg/mL) to slow down the adsorption process. QCM-D measurements with this concentration show that the ΔD response is downscaled in time by a factor of 50, while the salient features, such as the maximum and the relative minimum values, remain unchanged (Figure 1b, pH = 7.3). We therefore conclude that the kinetics of the process slow down with the concentration of Lf, while the mode of formation of the layer remains the same. It has to be stressed at this point that the behavior of the QCM signal, with a dissipation maximum at an early adsorption stage as reported in this study, must not be mistaken for the transient response that was frequently observed in older-generation QCM instruments when the solution is changed. The dependence of the time scale of this effect on the protein concentration and the fact that it was not observed with other proteins (fibronectin, bovine serum albumin, and lysozyme were also tested[9]) as well as the general absence of such artifacts in the data obtained with the QCM-D E4 confirm that it is correlated with the adsorption of Lf on the sample.

For the AFM measurements, PAA-coated Si samples were immersed into protein solutions with 1 μg/mL of Lf at the same pH values as before and subsequently analyzed with the AFM to investigate the morphology of the adsorbed protein layer at different stages. The AFM images obtained under these conditions at pH 7.3 for deposition times of 10, 20, 40 and 120 min are shown in Figure 2. Here, the image in Figure 2a (5 μm × 5 μm) corresponds to a stage where the dissipation is in the initial stage of sharp increase, Figure 2b (5 μm × 5 μm) corresponds to the maximum in dissipation, Figure 2c (25 μm × 25 μm) to the steep decrease after the maximum, and finally Figure 2d (25 μm × 25 μm) is already beyond the relative dissipation minimum.

It is immediately obvious that the adsorbed proteins do not form a homogeneous layer but rather condense to individual droplets on the PAA surface. Quantitative evaluation of the relative surface area A/A_0 covered by droplets (Figure 1c) reveals that there is a maximum that corresponds to the maximum of the dissipation. In addition, the maximum number of droplets per unit area (35 ± 4 droplets per μm^2) also corresponds to the maximum of the dissipation shift. It can therefore be concluded

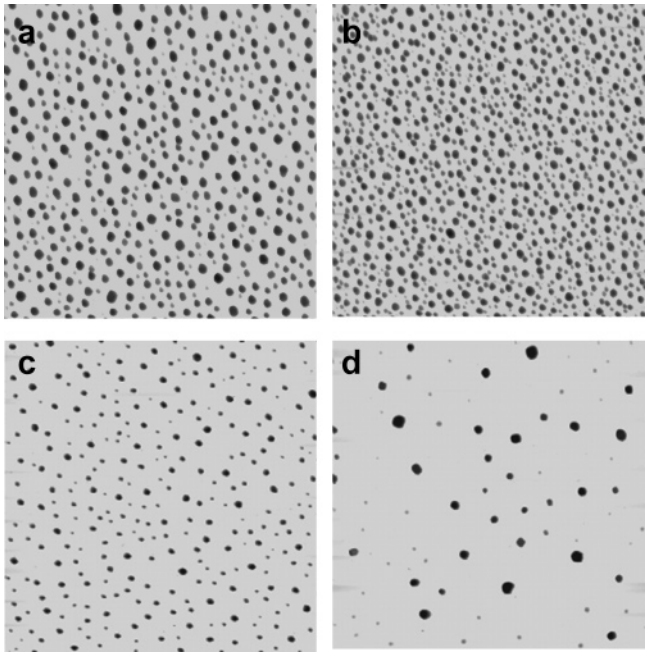

Figure 2. AFM images obtained after immersion of PAA covered SiO_2/Si samples in 1 μg/mL Lf solution in PBS at pH 7.3 for (a) 10 min, (b) 20 min, (c) 40 min, and (d) 120 min. Image sizes: (a,b): 5×5 μm^2, (c,d) 25×25 μm^2. The contrast in the images is reversed, i.e., protein droplets appear as dark areas.

that there are three regions of droplet formation in this system: (i) The nucleation of droplets is the main process up to a certain coverage. That region can be associated with the initial steep increase of the dissipation (Figure 1a,b). Subsequently, (ii) the droplets start to coagulate into larger drops, and the number of droplets and the dissipation decrease, although the adsorption of Lf molecules continues. After the minimum of the dissipation is reached, (iii) the system switches from coagulation to ripening, where the droplets continue to grow, probably mainly by Ostwald ripening, but also by additional adsorption of molecules from the solution. Between the dissipation minimum and saturation, Δf changes only by 5%. The dissipation continues to increase slightly, caused by growth of the droplets due to ripening.

At each adsorption stage, several measurements were made at different positions of the samples to ensure that the droplets are distributed homogeneously. Such measurements were also made by AFM directly on the PAA-functionalized QCM sensors after exposure to Lf in the flow cells. Those results also showed a homogeneous droplet distribution, which indicates that under our experimental conditions, the flow did not induce any inhomogeneity in the distribution of the droplets.

To quantitatively relate the topographic information obtained from the AFM measurements to the viscoelastic data from the QCM, we apply a modified viscoelastic model.[10−12] Starting from equivalent circuit models, a quartz crystal can be characterized by its complex acoustic impedance Z_q^*. The response of such a quartz crystal upon additional loading can be generally written in terms of a complex impedance Z^* of the loading material, which leads to a complex frequency shift Δf_n^* of its nth overtone. The complex frequency shift is related to the acoustic impedance Z^* of the loading material by[10,15,16]

$$\Delta f_n^* = \frac{i f_0}{\pi} \cdot \frac{Z^*}{Z_q} = \Delta f_n + i\Delta\Gamma_n \qquad (1)$$

Here, f_0 is the fundamental frequency and $Z_q = \sqrt{\rho_q G_q}$ is the acoustic impedance of the quartz where the density and the shear modulus of the quartz are ρ_q and G_q, respectively. In the more general representation at the right side of expression (1), the real part, Δf_n, is the change in resonance frequency and the imaginary part, $\Delta\Gamma_n$, is the shift of the half-band bandwidth ("bandwidth"). The bandwidth Γ of the nth resonance frequency, f_n, is often expressed in terms of a quality factor Q_n or a dissipation factor D_n, where the latter is the sum of the energy dissipation in the oscillating system. D_n, Q_n, and Γ_n are related to each other by[17]

$$Q_n = \frac{1}{D_n} = \frac{f_n}{2\Gamma_n} \qquad (2)$$

Hence, a change in the bandwidth, for instance by formation of a viscoelastic layer, can be related to a change in the dissipation by $\Delta D_n = (2\Delta\Gamma_n)/(f_n + \Delta f_n)$.

In the last expression, the frequency shift Δf_n can be neglected if the load is small compared to the mass of the crystal. If the thickness of the crystal is much larger than the decay length of the acoustic shear wave in the material, Z^* can be written in terms of the complex elastic shear modulus, G_v^*, and the density, ρ_v, of the viscoelastic load as $Z^* = \sqrt{\rho_v G_v^*} = \sqrt{\rho_v |G^*|} \cdot e^{i\phi/2}$. Here, $|G^*|$ and ϕ are, respectively, the magnitude and the phase angle of G_v^*.

To account for a nonuniform coverage of the quartz crystal (by droplets, for instance), a viscoelastic model adapted to this situation has to be applied.[11,18] According to that model, the sensitivity of the QCM is determined by the ratio of the loaded area A to the total active area A_0, and a sensitivity factor K_A that accounts for the variation of the shear oscillation amplitude across the surface of the quartz. With this and the above expression for Z^*, Δf_n^* can be expressed as

$$\Delta f_n^* = \frac{i f_0}{\pi \cdot Z_q} \cdot \sqrt{\rho_v |G^*|} \cdot e^{i\phi/2} \cdot K_A \frac{A}{A_0}$$

K_A is defined as $K_A = (A_0)/(A) \cdot (\int_0^a u^2(r) 2\pi r \, dr / \int_0^{r_0} u^2(r) 2\pi r \, dr)$, i.e., A_0/A multiplied by the ratio of the integrated squared surface shear displacement $u(r)$ across the contact area ($r = a$) to the same integral evaluated over the entire active surface of the quartz crystal ($r = r_0$). The shear displacement amplitude $u(r)$ can be approximated by the function $u(r) = u_{max} \exp(-\beta(r^2)/(r_0^2))$, where β is a factor which is close to 1.

Using the latter expression for $u(r)$ in the integrals, and by replacing r_0 by ∞ (because $u(r)$ decays rapidly for $r > r_0$), the constant K_A can be evaluated as $K_A \cdot (A)/(A_0) = 1 - \exp(-2\beta(A)/(A_0))$. Z^* is replaced by $\Delta Z^* = Z_2^* - Z_1^*$ if the quartz crystal is submerged into a (generally viscoelastic) liquid 1 and then covered in part by another viscoelastic liquid 2, which is in contact with the electrode over an area A. In this case, Δf_n^* depends on the properties of both liquids 1 and 2 because the acoustic impedance as sensed by the QCM changes. With this, we get

$$\Delta f_n^* = \frac{i f_0}{\pi \cdot Z_q} \cdot (Z_2^* - Z_1^*) \cdot \left(1 - \exp\left(-2\beta \frac{A}{A_0}\right)\right)$$

This expression can be separated into a real and an imaginary part, which represent $\Delta f_n$and $\Delta\Gamma_n$, respectively, by using Euler's relation. We now assume that liquid 1 is purely viscous (Newtonian). For such a liquid, the phase angle of the complex shear modulus G_1^* is $\phi_1 = 90°$, and its magnitude is $|G_1^*| = 2\pi f_n \eta_1$, where η_1 is the Newtonian viscosity of liquid 1. Hence,

for the case of droplets of a viscoelastic liquid 2 on a QCM sensor immersed in a Newtonian liquid 1, in our case, a highly diluted protein solution, we can write for $\Delta\Gamma_n$:[12]

$$\Delta\Gamma_n = \frac{f_0}{\pi \cdot Z_q} \cdot \left(1 - \exp\left(-2\beta \frac{A}{A_0}\right)\right)[\sqrt{\rho_{v2}|G_2^*|}\cos(\phi_2/2) - \sqrt{\pi f_n \rho_1 \eta_1}] \quad (3)$$

To apply this model to our experimental results, we determine the change in dissipation ΔD after 10, 20, 40, and 120 min (Figure 1b). These values are plotted vs the relative surface A/A_0 covered by the droplets at the same adsorption times (Figure 1c). In the resulting plot (Figure 1d), the adsorption time is now eliminated. Note that, in this case, the Lf concentration (1 μg/mL), pH value, and temperature are the same for the AFM and QCM experiments.

For the very high dilution of 1 μg/mL Lf in PBS, we can safely assume that this solution is a purely Newtonian fluid with $\phi_1 = 90°$ so that eq 3 can be applied, with $\rho_1 = 1.0$ g/cm^3 and $\eta_1 = 1.0$ mPa·s, the same as for water. $f_n = 15$ MHz, i.e., the third harmonics of a quartz sensor with $f_0 = 5$ MHz, while its acoustic impedance Z_q can be calculated from the quartz density $\rho_q = 2.65$ g/cm^3 and its shear modulus $G_q = 1.95 \times 10^{10}$ Pa. With these values, and taking into account the relation between ΔD and $\Delta\Gamma_n$, eq 3 can be fitted to the data using a droplet density of $\rho_{v2} = 1.1$ g/cm^3, a shear modulus of $|G_2^*| = 8.39 \times 10^4$ Pa and a phase angle of $\phi_2 = 88°$. A density of the droplet material of 1.1 g/cm^3 is reasonable because it can be considered as highly concentrated aqueous solution of Lf. Hence its density should be higher than that of water, but at the same time considerably lower than 1.35 g/cm^3, the widely used average value for pure proteins with a molecular weight larger than 20 kDa.[19] The shear modulus of 83.9 kPa is well within the range found for solutions of proteins with a similar weight,[20] and a phase angle slightly below 90° is indicative of a predominantly viscous liquid with a relatively weak elastic character. A reasonable fit to the experimental data can also be obtained by slight variation of ρ_{v2}, $|G_2^*|$ and ϕ_2, but it was not possible to get such a fit for significantly different values.

The best fit to the experimental data is obtained with $\beta = 1.2$ in eq 3, and this is drawn in Figure 1d as a solid line. The results for $\beta = 1.0$ and $\beta = 1.4$ are included in that figure as dashed lines. This analysis shows that the formation of droplets by adsorption of Lf on PAA from an aqueous solution can be well described with the viscoelastic model discussed above. The small deviation of the experimental data from the fit (the first two points above the curve for $\beta = 1.2$, the next two points below it) could be due to the factor β, which was assumed to be constant in the discussion above, but may as well be weakly dependent on A/A_0.

Figure 1d also shows that ΔD increases with the contact area A/A_0. This is the reason for the decrease of ΔD in the coagulation regime of the droplets (i. e., the decrease of ΔD after the maximum in the ΔD vs *time* plot in Figure 1a,b), where the total contact area of the aggregates with the surface decreases. Only when A/A_0 increases again by continuous adsorption of molecules from the solution, the minimum in ΔD is passed and the dissipation increases again.

Droplet or aggregate formation instead of spreading of the protein layer indicates that the interaction between the PAA surface and Lf is relatively weak under our experimental conditions. Additional ζ potential measurements show that most of the carboxylic acid groups of the PAA surface are dissociated and the surface is negatively charged at pH > 7.[9] However, the adsorption was carried out under conditions that minimize the Coulomb interaction between the protein and the PAA surface, i.e., at pH values in the vicinity of the isoelectric point (pI) of Lf (which is around pH 8), where the molecules carry little excess charge. On the other hand, the regions and density of negative charges on the Lf surface tend to increase at pH close to the pI of the protein, which enhances intermolecular electrostatic attraction between the oppositely charged regions on the Lf surface.[21] This reduced interaction between Lf and PAA and the enhanced intermolecular attraction in the vicinity of pH 8, in addition to possible other noncovalent attractive interactions, favors droplet formation rather than spreading of the protein, where the latter would result in a more homogeneous film. Moreover, the fact that, at low pH values, the characteristic maximum in the dissipation is absent points toward the formation of a more homogeneous layer under those conditions. At low pH values, the Lf molecules carry excess positive charge, while the ζ potential of PAA is still negative,[9] which indicates that the surface carries a negative electric charge. Under those conditions, a maximum of the covered surface A/A_0 was not observed with the AFM, implying that the interaction between Lf and the surface is strong enough to prevent the formation of large Lf droplets on the surface.

In conclusion, we have analyzed the formation of droplets during the adsorption of Lf on plasma-deposited PAA. At pH values close to the pI of Lf, the interaction between the molecules and the PAA-functionalized surface is weak in comparison to the intermolecular attraction. This leads to droplet formation rather than to a homogeneous film. The dynamic properties of such a system can be described within a viscoelastic model that explicitly takes the nonhomogeneity of the adsorbed layer into account.

References and Notes

(1) Castner, D. G.; Ratner, B. D. *Surf. Sci.* **2002**, *500*, 28.
(2) Kasemo, B. *Surf. Sci.* **2002**, *500*, 656.
(3) Willner, I.; Katz, E. *Bioelectronics*; Wiley-VCH: Weinheim, 2005.
(4) Gordon, L. *Biosensors and Modern Biospecific Analytical Techniques*; Elsevier: Amsterdam, 2005.
(5) Keller, C. A.; Glasmästar, K.; Zhdanov, V. P.; Kasemo, B. *Phys. Rev. Lett.* **2000**, *84*, 5443.
(6) Rodahl, M.; Höök, F.; Fredriksson, C.; Keller, C. A.; Krozer, A.; Brzezinski, P.; Voinova, M. V.; Kasemo, B. *Faraday Discuss.* **1997**, *107*, 229.
(7) Reimhult, E.; Höök, F.; Kasemo, B. *Langmuir* **2003**, *19*, 1681.
(8) Persson, B. *Sliding Friction*; Springer: Berlin, 1997.
(9) Belegrinou, S.; Mannelli, I.; Bretagnol, F.; Valsesia, A.; Sirghi, L.; Ceccone, G.; Rossi, F.; Rauscher, H. to be published.
(10) Johannsmann, D. *Macromol. Chem. Phys.* **1999**, *200*, 501.
(11) Flanigan, C. M.; Desai, M.; Shull, K. R. *Langmuir* **2000**, *16*, 9825.
(12) Nunalee, F. N.; Shull, K. R.; Lee, B. P.; Messersmith, P. B. *Anal. Chem.* **2006**, *78*, 1158.
(13) Lejeune, M.; Valesia, A.; Kormunda, M.; Colpo, P.; Rossi, F. *Surf. Sci.* **2005**, *583*, L142.
(14) Voinova, M. V.; Rodahl, M.; Jonson, M.; Kasemo, B. *Phys. Scr.* **1999**, *59*, 391.
(15) Johannsmann, D.; Mathauer, K.; Wegner, G.; Knoll, W. *Phys. Rev. B* **1992**, *46*, 7808.
(16) Bund, A.; Chmiel, H.; Schwitzgebel, G. *Phys. Chem. Chem. Phys.* **1999**, *1*, 3933.
(17) Johannsmann, D.; Heim, L.-O. *J. Appl. Phys.* **2006**, *100*, 0945051.
(18) König, A.; Düwel, M.; Du, B.; Kunze, M.; Johannsmann, D. *Langmuir* **2006**, *22*, 229.
(19) Fischer, H.; Polikarpov, I.; Craievich, A. F. *Protein Sci.* **2004**, *13*, 2825.
(20) Naumenko, A. V.; Kovalev, G. N.; Naumanko, V. Y.; Zaraisky, E. I.; Snegireva, N. S. *Biophysics* **2006**, *51*, 209.
(21) Ye, A.; Singh, H. *J. Colloid Interface Sci.* **2006**, *295*, 249.